

Synthesis, characterization, and morphological control of $\text{Eu}_2\text{Ti}_2\text{O}_7$ nanoparticles through green method and its photocatalyst application

Ali Sobhani-Nasab¹ · Mohsen Behpour¹

Received: 3 May 2016 / Accepted: 9 July 2016 / Published online: 25 July 2016
© Springer Science+Business Media New York 2016

Abstract Nowadays, in connection with the increasing pollution of the environment, several studies are performed in order to find new group of compounds which could replace chemical synthesis capping agents due to their high toxicity to ecosystem and difficulty in being degraded in the environment. In the current study, an attempt is made to synthesize europium titanate ($\text{Eu}_2\text{Ti}_2\text{O}_7$) nanoparticles through a green method with the aid of natural capping agents such as glucose, fructose, galactose, lactose and starch in an aqueous solution and investigate their effect on the morphology and particle size of final products. According to the vibrating sample magnetometer result, $\text{Eu}_2\text{Ti}_2\text{O}_7$ nanoparticles indicated a paramagnetic behavior at room temperature. In addition, methyl orange was chosen as a dye water pollution to evaluate its degradation by as-synthesize $\text{Eu}_2\text{Ti}_2\text{O}_7$ nanoparticles under ultraviolet light irradiation. Furthermore, the photocatalysis results reveal that the maximum decolorization of 94 % for methyl orange occurred with $\text{Eu}_2\text{Ti}_2\text{O}_7$ nanoparticles in 60 min under ultraviolet light irradiation.

1 Introduction

There has been considerable interest in the preparation of semiconductor nanostructures and the investigation of their properties in the past decade [1–5]. The removal of dyes and toxic organic compounds from wastewater has been studied widely and has attracted more attention as cleaner and

greener technology; hence, in the past few decades, high efficiency and stable photocatalytic materials have been extensively studied for the degradation of organic pollutants and developed their potential applications to environmental remediation [6–9]. Lanthanide titanium oxides, which crystallize in a pyrochlore structure with general formula $\text{RE}_2\text{Ti}_2\text{O}_7$ (RE = rare earth element) [10], have been extensively investigated in recent years for their interesting physical and chemical properties. Their physical properties depend mainly on the rare earth element incorporated inside their crystal lattice. According to theoretical predictions they exhibit exciting magnetic properties [11, 12]. For example, compounds of Dy or Ho exhibit the magnetic properties of a spin-ice [12], anti-ferromagnetic properties are observed in the case of Er and Gd [11], and compounds of Eu exhibit highly constant magnetic susceptibility [13]. Despite the poor luminescence of the pyrochlore structure, they also find their place in the field of optical materials. Compounds of $\text{Y}_2\text{Ti}_2\text{O}_7$ doped with Er and Yb have been proposed as attractive novel materials for lasers and optical amplifiers [14, 15]. Besides, their applications in the electronics industry, pyrochlores have demonstrated their abilities as catalysts [16] and as novel materials for hydrogen storage cells [17]. Such advanced applications place high demands on the quality of the prepared material. Various methods that lead to the formation of $\text{RE}_2\text{Ti}_2\text{O}_7$ with tailored properties have been reported. Monocrystals are routinely prepared by a flux technique [18] or a floating zone technique [19] while polycrystalline materials are usually prepared by solid-state reactions [20] or wet-chemical approaches [14, 15, 21, 22]. In this study, sol-gel method is performed to synthesize and characterize $\text{Eu}_2\text{Ti}_2\text{O}_7$ nanoparticles. In addition, five natural capping agents such as glucose, fructose, galactose, lactose, and starch which called carbohydrates, were applied and their effects on the morphology and particle size of final

✉ Mohsen Behpour
m.behpour@kashanu.ac.ir

¹ Institute of Nano Science and Nano Technology, University of Kashan, P.O. Box 87317-51167, Kashan, I. R. Iran

products were investigated. This approach is simple, low energy consumption and friendly to the environment. A green approach for $\text{Eu}_2\text{Ti}_2\text{O}_7$ nanoparticles synthesis by utilizing natural template permits the reaction to proceed usually in milder conditions. Although existing chemical approaches have effectively produced well-defined $\text{Eu}_2\text{Ti}_2\text{O}_7$ nanoparticles, these processes are generally costly and include the employ of toxic chemicals. Moreover, the photocatalytic degradation was investigated using methyl orange (MO) under ultraviolet light irradiation to study the photocatalytic activity of as-prepared nanoparticles.

2 Experimental

2.1 Characterization

X-ray diffraction (XRD) pattern was recorded by a Philips-X'PertPro, X-ray diffractometer using Ni-filtered $\text{Cu K}\alpha$ radiation at scan range of $10 < 2\theta < 80$. Scanning electron microscopy (SEM) images were obtained on LEO-1455VP equipped with an energy dispersive X-ray spectroscopy. The electronic spectra were obtained on a Scinco UV-Vis scanning spectrometer (Model S-10 4100). The energy dispersive spectrometry (EDS) analysis was studied by XL30, Philips microscope. The magnetic measurement of sample was carried out in a vibrating sample magnetometer (VSM) (Meghnatis Daghigh Kavir Co.; Kashan Kavir; Iran) at room temperature.

2.2 Synthesis of $\text{Eu}_2\text{Ti}_2\text{O}_7$ nanoparticles

The carbohydrates, europium salt, ethanol, and tetra-*n*-butyl titanate (TNBT) were purchased from Merck Company and used without further purification. At first, a stoichiometric amount of TNBT and europium nitrate (1:1) was separately dissolved in ethanol in two beakers A and B, respectively. Then, carbohydrates as the capping agents were dissolved in ethanol and added to the A solution under constant stirring. Afterwards, the $\text{Eu}(\text{NO}_3)_3 \cdot 6\text{H}_2\text{O}$ solution was mixed with above mentioned solution under stirring at room temperature. Subsequently, the final mixed solution was kept stirring to form a gel at 90 °C. Finally, the obtained product was calcinated at 900 °C temperatures for 3 h in a conventional furnace in air atmosphere. Reaction conditions are listed in Table 1.

2.3 Photocatalytic experimental

The methyl orange (MO) photodegradation was examined as a model reaction to evaluate the photocatalytic activities of the $\text{Eu}_2\text{Ti}_2\text{O}_7$ nanoparticles under ultraviolet light irradiations. The photocatalytic degradation was performed

with 150 mL solution of methyl orange (0.0005 g) containing 0.05 g of $\text{Eu}_2\text{Ti}_2\text{O}_7$. This mixture was aerated for 30 min to reach adsorption equilibrium. Later, in order to perform photocatalytic tests, the mixture was placed inside the photoreactor in which the vessel was 15 cm away from the ultraviolet source of 400 W mercury lamps at room temperature. Aliquots of the mixture were taken at definite interval of times during the irradiation and after centrifugation they were analyzed by a UV-Vis spectrometer. The methyl orange (MO) degradation percentage was calculated as:

$$\text{Degradation rate (\%)} = \frac{A_0 - A}{A_0} \times 100 \quad (1)$$

where A_0 and A are the absorbance value of solution at A_0 and A min, respectively.

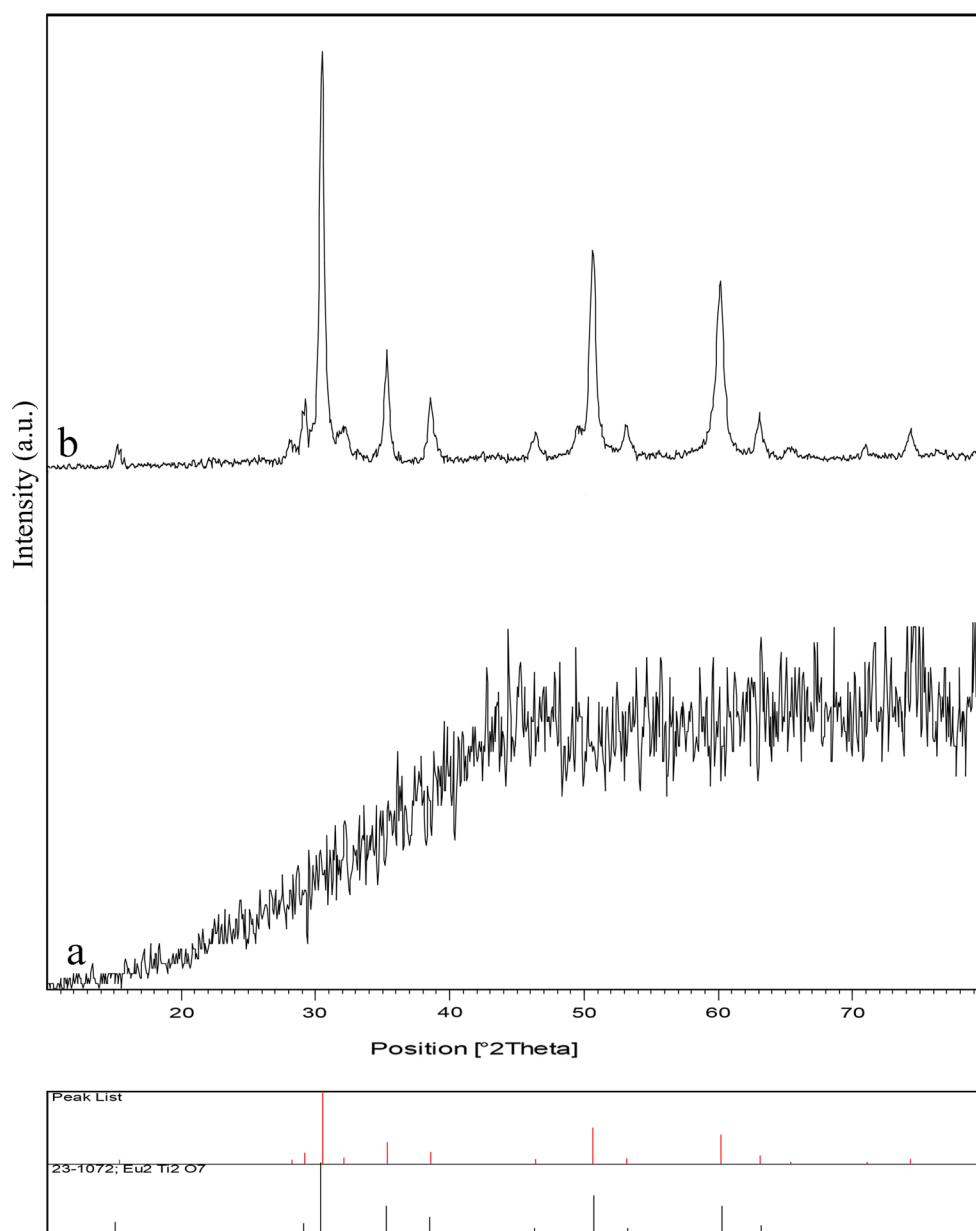
3 Results and discussion

Crystalline structure and phase purity of as-prepared products, before and after calcination, have been determined using XRD. The XRD patterns of as-prepared $\text{Eu}_2\text{Ti}_2\text{O}_7$ sample 1 before and after calcination are shown in Fig. 1a, b, respectively. In the absence of calcination at 900 °C, $\text{Eu}_2\text{Ti}_2\text{O}_7$ is amorphous, as shown in Fig. 1a. Based on the Fig. 1b, the diffraction peaks observed can be indexed to pure cubic phase of $\text{Eu}_2\text{Ti}_2\text{O}_7$ ($a = b = c = 10.1930 \text{ \AA}$) with space group of $Fd-3m$ and JCPDS No. 23-1072, in calcination at 900 °C. No diffraction peaks from other species could be detected, which indicates the obtained sample is pure. From XRD data, the crystallite diameter (D_c) of $\text{Eu}_2\text{Ti}_2\text{O}_7$ nanoparticles (sample 1) was calculated to be 22 nm using the following Scherer equation:

$$D_c = K\lambda/\beta \cos \theta$$

where β is the breadth of the observed diffraction line at its half intensity maximum, K is the so-called shape factor, which usually takes a value of about 0.9, and λ is the wavelength of X-ray source used in XRD. In recent years, growing interesting in control morphology and particle size of final products thanks to the benefit from different reaction conditions has been one of the main areas of research [23–31]. In addition, capping agents as an inseparable part of synthesis nanomaterials give a great chance to researchers to focus on different type of capping agents such as anionic, cationic, natural, and etc to control morphology and particle size of final products; therefore, in the presence study, effects of several natural carbohydrates capping agents such as glucose, fructose, galactose, lactose and starch on the morphology and particle size of final products were investigated. Morphology and particle size of $\text{Eu}_2\text{Ti}_2\text{O}_7$ in the presence of different natural

Fig. 1 XRD pattern of $\text{Eu}_2\text{Ti}_2\text{O}_7$ nanoparticles sample 1, *a* before calcination, *b* after calcinations



carbohydrates capping agents were investigated by SEM images, as shown in Fig. 2. According to the Fig. 2a–e, all samples are mainly consisting of nanoparticles with average particle size 30–50 nm. Furthermore, starch causes particles to agglomerate. Since in this study capping agents were used; therefore, the EDS analysis measurement was used to investigate the chemical composition and purity of $\text{Eu}_2\text{Ti}_2\text{O}_7$ nanoparticles (sample 1), as shown in Fig. 3. According to the Fig. 3, the product consists of Eu, Ti, and O elements. Furthermore, neither N nor C signals were detected in the EDS spectrum, which means the product is pure and free of any surfactant or impurity. The VSM magnetic measurement was used to measure the magnetic property of $\text{Eu}_2\text{Ti}_2\text{O}_7$ nanoparticle (sample 1, Fig. 4). The

$\text{Eu}_2\text{Ti}_2\text{O}_7$ nanoparticle (sample 1) exhibits paramagnetic behavior at room temperature with a saturation magnetization of 0.16 emu/g. The diffused reflectance spectrum of the as-prepared $\text{Eu}_2\text{Ti}_2\text{O}_7$ nanoparticles is shown in Fig. 5. The fundamental absorption edge in most semiconductors follows the exponential law. Using the absorption data the band gap was estimated by Tauc's relationship:

$$\alpha = \alpha_0(h\nu - E_g)^n/h\nu \quad (2)$$

where α is absorption coefficient, $h\nu$ is the photon energy, α_0 and h are the constants, E_g is the optical band gap of the material, and n depends on the type of electronic transition and can be any value between $\frac{1}{2}$ and 3. The energy gap of the $\text{Eu}_2\text{Ti}_2\text{O}_7$ nanoparticles (sample 1) is determined by

Fig. 2 SEM images of $\text{Eu}_2\text{Ti}_2\text{O}_7$ nanoparticles **a** sample 1, **b** sample 2, **c** sample 3, **d** sample 4, **e** sample 5

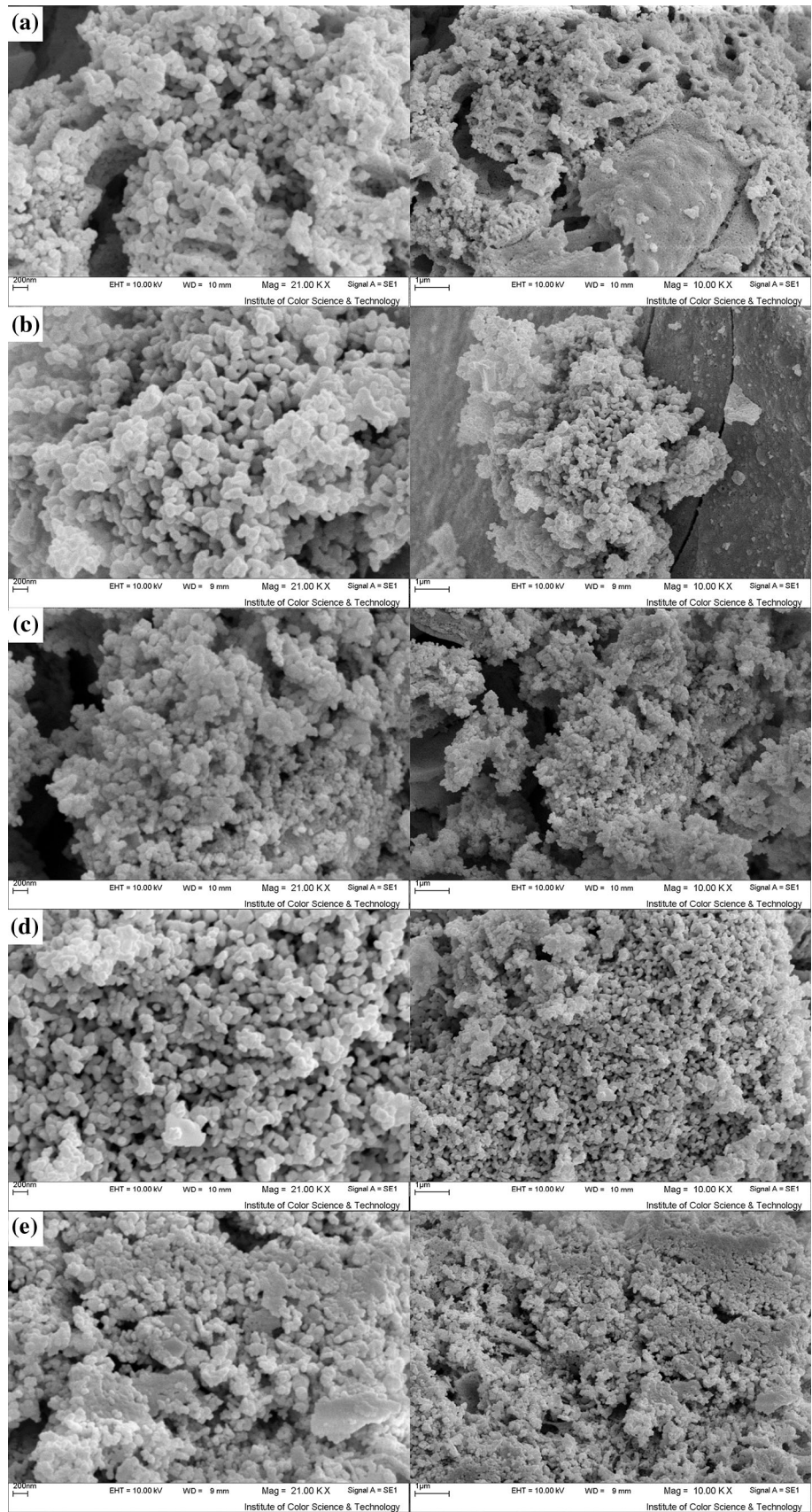
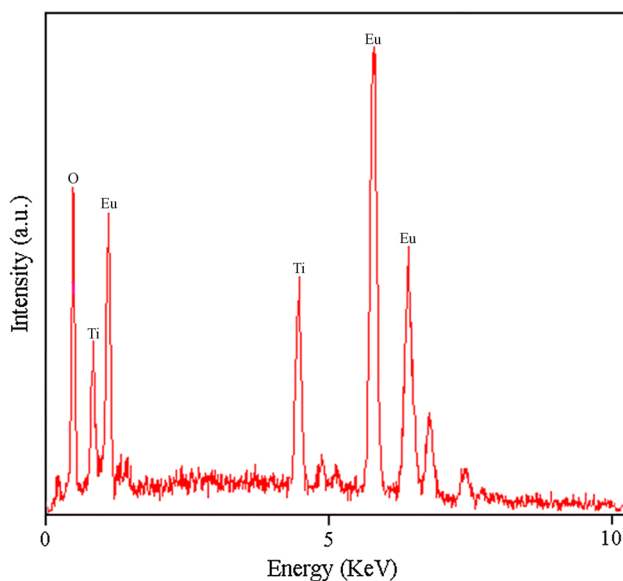
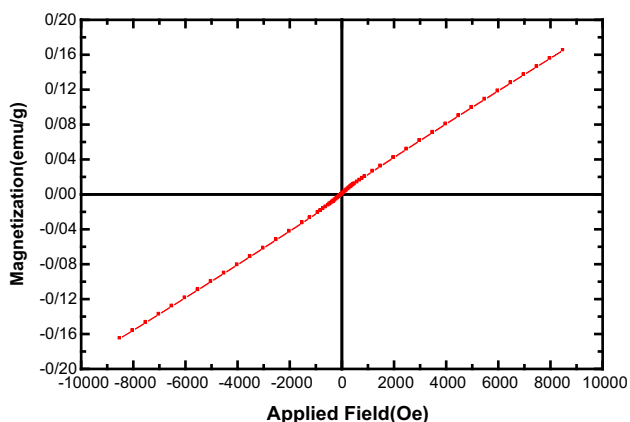
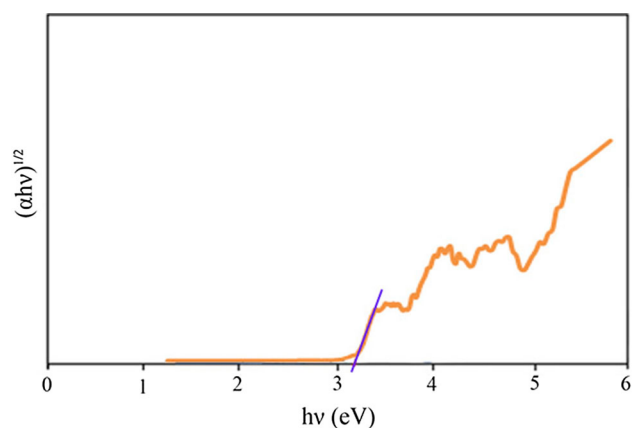
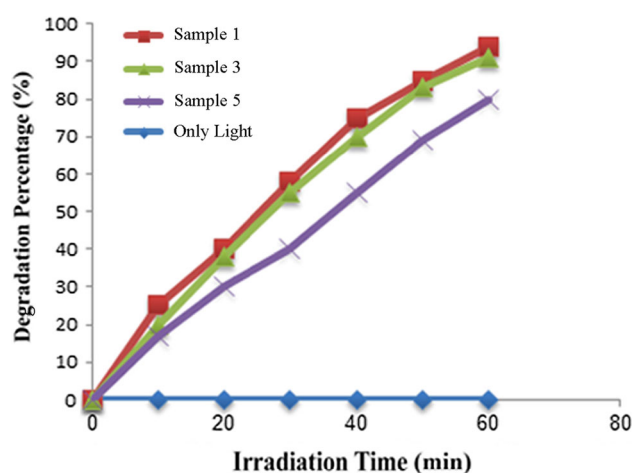


Table 1 Reaction conditions for $\text{Eu}_2\text{Ti}_2\text{O}_7$ nanoparticles

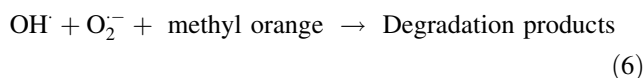
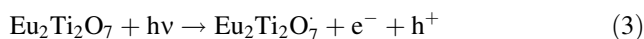
Sample no.	Temperature	Surfactant	Degradation (%)
1	900	Glucose	94
2	900	Fructose	–
3	900	Galactose	91
4	900	Lactose	–
5	900	Starch	81

**Fig. 3** EDS pattern of $\text{Eu}_2\text{Ti}_2\text{O}_7$ nanoparticles (sample 1)**Fig. 4** VSM curve of $\text{Eu}_2\text{Ti}_2\text{O}_7$ nanoparticles (sample 1)

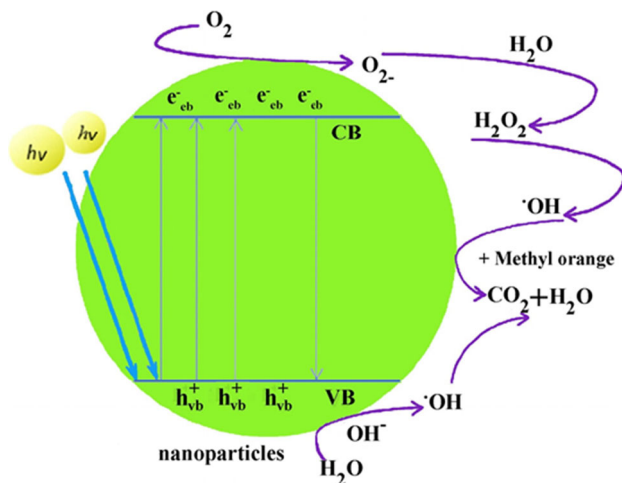
extrapolating the linear portion of the plots of $(\alpha h\nu)^{1/2}$ against $h\nu$ to the energy axis, as shown in Fig. 5. The E_g value is calculated as 3.2 eV for the $\text{Eu}_2\text{Ti}_2\text{O}_7$ nanoparticles. Photodegradation of methyl orange (MO) solution under UV light illumination was employed to evaluate the photocatalyst properties of the as-synthesized $\text{Eu}_2\text{Ti}_2\text{O}_7$

**Fig. 5** Tauc plot pattern of $\text{Eu}_2\text{Ti}_2\text{O}_7$ nanoparticles (sample 1)**Fig. 6** Photocatalytic methyl orange degradation of $\text{Eu}_2\text{Ti}_2\text{O}_7$ nanoparticles (samples 1, 3 and 5) under ultraviolet light

nanoparticles (samples 1, 3, and 5, Fig. 6). No methyl orange was practically broken down after 60 min in the absence of as-prepared $\text{Eu}_2\text{Ti}_2\text{O}_7$ nanoparticles. The proposed mechanisms of the photocatalytic degradation of the methyl orange with the aid of $\text{Eu}_2\text{Ti}_2\text{O}_7$ nanoparticles can be assumed as:



Utilizing photocatalytic calculations by Eq. (1), the methyl orange degradation was about 94 % after 60 min illumination of UV light in the presence of $\text{Eu}_2\text{Ti}_2\text{O}_7$ nanoparticles (sample 1). Besides, the whole mechanism is shown in Scheme 1.



Scheme 1 Reaction mechanism of methyl orange photodegradation over $\text{Eu}_2\text{Ti}_2\text{O}_7$ nanoparticles under UV light irradiation

4 Conclusions

In this work, $\text{Eu}_2\text{Ti}_2\text{O}_7$ nanoparticles were successfully synthesized through a green method in an aqueous solution. EDS and XRD results proved high purity of the as-prepared $\text{Eu}_2\text{Ti}_2\text{O}_7$ nanoparticles. In order to investigate the effect of several natural carbohydrates capping agents on the morphology and particle size of final products several tests were performed in the presence of glucose, fructose, galactose, lactose and starch. Applying nanocrystalline $\text{Eu}_2\text{Ti}_2\text{O}_7$ as the photocatalyst causes maximum 94 % degradation of methyl orange after 60 min irradiation of UV light. This result suggests that as-obtained nanocrystalline $\text{Eu}_2\text{Ti}_2\text{O}_7$ as favorable material has high potential to be used for photocatalytic applications under UV light.

Acknowledgments Authors are grateful to council of University of Kashan for providing financial support to undertake this work.

References

1. S.M. Hosseinpour-Mashkani, M. Ramezani, A. Sobhani-Nasab, M. Esmaili-Zare, *J. Mater. Sci. Mater. Electron.* **26**, 6086 (2015)
2. A. Sobhani-Nasab, M. Maddahfar, S.M. Hosseinpour-Mashkani, *J. Mol. Liq.* **216**, 1 (2016)
3. M. Behpour, M. Mehrzad, S.M. Hosseinpour-Mashkani, *J. Nanostruct.* **5**, 183 (2015)
4. J. Safari, Z. Zarnegar, *J. Nanostruct.* **3**, 191 (2013)
5. J. Safaei-Ghomi, S. Zahedi, M. Javid, M.A. Ghasemzadeh, *J. Nanostruct.* **5**, 153 (2015)
6. M. Enhessari, M. Kargar-Razi, P. Moarefi, A. Parviz, *J. Nanostruct.* **2**, 119 (2012)
7. S. Khaleghi, *J. Nanostruct.* **2**, 157 (2012)
8. M. Behpour, M. Chakeri, *J. Nanostruct.* **2**, 227 (2012)
9. S. Farhadi, F. Siadatnasab, K. Jahanara, *J. Nanostruct.* **3**, 227 (2013)
10. R.A. McCauley, *J. Appl. Phys.* **51**, 290 (1980)
11. J.D.M. Champion, M.J. Harris, P.C.W. Holdsworth, A.S. Wills, G. Balakrishnan, S.T. Bramwell, E. Cizmar, T. Fennell, J.S. Gardner, J. Lago, D.F. McMorro, M. Orendac, A. Orendacova, D.M. Paul, R.I. Smith, M.T.F. Telling, A. Wildes, *Phys. Rev. B* **68**, 020401 (2003)
12. R. Siddharthan, B.S. Shastry, A.P. Ramirez, A. Hayashi, R.J. Cava, S. Rosenkranz, *Phys. Rev. Lett.* **83**, 1854 (1999)
13. S. Zouari, R. Ballou, A. Cheikh-Rouhou, P. Strobel, *Mater. Lett.* **62**, 3767 (2008)
14. P. Jenouvrier, G. Boccardi, J. Fick, A.M. Jurdy, M. Langlet, *J. Lumin.* **113**, 291 (2005)
15. M. Langlet, P. Jenouvrier, J. Fick, R. Rimet, *J. Sol-Gel. Sci. Technol.* **26**, 985 (2003)
16. Y.Q. Zhang, Y. Xuan, S.S. Qian, X.L. Li, Y.Q. Jia, *J. Mater. Sci.* **34**, 4475 (1999)
17. L. Zhang, W. Zhang, J. Zhu, Q. Hao, C. Xu, X. Yang, L. Lu, X. Wang, *J. Alloys Compd.* **480**, 45 (2009)
18. K.B. Helean, S.V. Ushakov, C.E. Brown, A. Navrotsky, J. Lian, R.C. Ewing, J.M. Farmer, L.A. Boatner, *J. Solid State Chem.* **177**, 1858 (2004)
19. M. Maczka, M.L. Sanjuan, A.F. Fuentes, L. Macalik, J. Hanuza, K. Matsuhira, Z. Hiroi, *Phys. Rev. B* **79**, 214437 (2009)
20. P. Holtappels, F.W. Poulsen, M. Mogensen, *Solid State Ion.* **135**, 675 (2000)
21. Z.M. Shao, S. Saitzek, P. Roussel, M. Huve, O. Desfeux, O. Mentre, F. Abraham, *J. Cryst. Growth* **311**, 4134 (2009)
22. M.R. Mohammadi, D.J. Fray, *Mater. Chem. Phys.* **122**, 512 (2010)
23. D. Ghanbari, M. Salavati-Niasari, S. Karimzadeh, S. Gholamrezaei, *J. Nanostruct.* **4**, 227 (2014)
24. M. Panahi-Kalamuei, M. Mousavi-Kamazani, M. Salavati-Niasari, *J. Nanostruct.* **4**, 459 (2014)
25. L. Nejati-Moghadam, A. Esmaili Bafghi-Karimabad, M. Salavati-Niasari, H. Safardoust, *J. Nanostruct.* **5**, 47 (2015)
26. S.M. Hosseinpour-Mashkani, M. Maddahfar, A. Sobhani-Nasab, *J. Mater. Sci. Mater. Electron.* **27**, 474 (2016)
27. S.S. Hosseinpour-Mashkani, S.S. Hosseinpour-Mashkani, A. Sobhani-Nasab, *J. Mater. Sci. Mater. Electron.* **27**, 4351 (2016)
28. M. Rahimi-Nasrabadi, M. Behpour, A. Sobhani-Nasab, S.M. Hosseinpour-Mashkani, *J. Mater. Sci. Mater. Electron.* **26**, 9776 (2015)
29. A. Sobhani-Nasab, M. Behpour, *J. Mater. Sci. Mater. Electron.* **27**, 1191 (2016)
30. S.M. Hosseinpour-Mashkani, A. Sobhani-Nasab, *J. Mater. Sci. Mater. Electron.* **27**, 3240 (2016)
31. A. Sobhani-Nasab, S.M. Hosseinpour-Mashkani, M. Salavati-Niasari, S. Bagheri, *J. Clust. Sci.* **26**, 1305 (2015)